20th IAEA Fusion Energy Conference
Vilamoura, Portugal, 1-6 November 2004

IAEA-CN-116/EX/6-1

Compatibility of Advanced Tokamak Plasma with High Density and High Radiation Loss Operation in JT-60U

H. Takenaga 1), N. Asakura 1), H. Kubo 1), S. Higashijima 1),
S. Konoshima 1), T. Nakano 1), N. Oyama 1), G. D. Porter 2),
T. D. Rognlien 2), M. E. Rensink 2), S. Ide 1), T. Fujita 1),
T. Takizuka 1), Y. Kamada 1), Y. Miura 1) and the JT-60 Team 1)

1) Japan Atomic Energy Research Institute, Naka-machi, Naka-gun, Ibaraki-ken, 311-0193, Japan
2) Lawrence Livermore National Laboratory, Livermore, CA 94551-9900, USA

Compatibility of Advanced Tokamak Plasma with High Density and High Radiation Loss Operation in JT-60U

H. Takenaga 1), N. Asakura 1), H. Kubo 1), S. Higashijima 1), S. Konoshima 1), T. Nakano 1), N. Oyama 1), G. D. Porter 2), T. D. Rognlien 2), M. E. Rensink 2), S. Ide 1), T. Fujita 1), T. Takizuka 1), Y. Kamada 1), Y. Miura 1) and the JT-60 Team 1)

1) Japan Atomic Energy Research Institute, Naka-machi, Naka-gun, Ibaraki-ken, 311-0193, Japan
2) Lawrence Livermore National Laboratory, Livermore, CA 94551-9900, USA

e-mail contact of main author : takenaga@naka.jaeri.go.jp

Abstract. Compatibility of advanced tokamak plasmas with high density and high radiation loss has been investigated in both reversed shear (RS) plasmas and high β_p H-mode plasmas with a weak positive shear on JT-60U. In the RS plasmas, the total radiation loss is enhanced to a level greater than 90% of the net heating power with high confinement (HH_{y2}=1.1) at a high density above the Greenwald density (n_{GW}) ($\bar{n}_e/n_{GW}$=1.1) by injecting seed impurity Ne together with D_2 gas. In the high β_p H-mode plasmas, high confinement (HH_{y2}=0.96) is maintained at high density ($\bar{n}_e/n_{GW}$=0.92) with high radiation loss fraction (f_{rad}>0.9) by utilizing high-field-side pellets and Ar injections. In both RS and high β_p H-mode plasmas, the high $\bar{n}_e/n_{GW}$ is obtained due to a peaked density profile inside the internal transport barrier (ITB). Strong core-edge parameter linkage is observed in the high β_p H-mode plasmas with the pellets and Ar injections, as well as without Ar injection. In this linkage, the pedestal β_p, defined as $\beta_p^{ped}=p^{ped}/(B_p^2/2\mu_0)$ where p^{ped} is the plasma pressure at the pedestal top, is enhanced with the total β_p. On the other hand, β_p^{ped} is kept at small value in the RS plasmas, indicating that confinement improvement is mainly attributed to the strong ITB. The radiation profile in the main plasma is peaked due to Ar accumulation inside the ITB in the high β_p H-mode plasmas. In the RS plasmas with Ne seeding, the radiation profile is also peaked in the main plasma, where the contribution of Ne to the radiation in the central region is small. The impurity transport analyses indicate that core radiation loss from Ar impurity more accumulated by a factor of 2 than the electron, as observed in the high β_p H-mode plasma, can be compensated with slightly enhanced confinement in a fusion reactor.

1. Introduction

Reversed and weak positive magnetic shear plasmas with internal transport barriers (ITBs) have been developed to establish an advanced steady-state operation scenario in fusion reactors such as ITER and SSTR [1]. These plasmas have advantages of compatibility with high bootstrap current fraction and high confinement, which are essential for the steady state operation. In order to apply these plasmas to fusion reactors, compatibility with high density and high radiation loss is also required for attaining the high fusion power and reducing the heat load localized onto the divertor plates. In the high density region, confinement degradation has been observed in the H-mode plasmas [2, 3]. In order to suppress the confinement degradation, sustainment of ITB is important in the high density region. High radiation loss in the divertor and scrape-off layer (SOL) plasmas enhanced by impurity seeding is most effective for expansion of the heat load onto the wide area [4, 5]. However, the heavy impurity accumulation has been observed inside the ITB [6, 7]. It is important to investigate applicability of the impurity seeding in the ITB plasmas.

In JT-60U, the reversed magnetic shear (RS) plasma and the high β_p H-mode plasma with a weak positive magnetic shear have been optimized to provide a physics basis for ITER and SSTR. The high confinement RS plasmas (HH_{y2}=1.4, where HH_{y2} is the confinement enhancement factor over the ITER98(y,2) scaling) have been achieved at ~80% of the Greenwald density (n_{GW}) under the full non-inductive current drive condition with a small radiation fraction [8]. In the high β_p H-mode plasmas, the high density of $\bar{n}_e/n_{GW}$=0.7 has been achieved with a radiation fraction of 60% using high-field-side (HFS) pellet injections [9]. In this plasma, core-edge parameter linkage plays an important role for confinement improvement, where the pedestal β_p is almost proportional to the total β_p. Further optimization for high density around or above n_{GW} and high radiation fraction greater than 80% is necessary to establish the steady state operation scenario. Since the heavy impurity such as argon (Ar) is accumulated inside the ITB [6], the seed impurity species should be selected from the viewpoint of suppression of the strong impurity accumulation. The radiation loss in the main plasma significantly increased with Ar seeding in the RS plasmas [10], while the radiation loss in the divertor plasma increased with neon (Ne) seeding. In the H-mode plasmas without the ITB, Ar seeding is effective for not only enhancement of the radiation loss but also the suppression of the confinement degradation at high density [11]. The Ar accumulation is weaker in the high β_p H-mode plasma than that in the RS plasma [6].

In this paper, impurity seeding using Ne is applied to the high density RS plasmas and impurity seeding using Ar is applied to high β_p H-mode plasmas. Extension of operation regime to high density and high radiation loss is presented in Sec. 2. In Sec. 3, core-edge linkage is discussed for confinement improvement at high density. The impurity transport and radiation profile are described in Sec. 4. Applicability of the impurity seeding to a fusion reactor is discussed in Sec. 5, followed by a summary in Sec. 6.

2. Extension of Operation Regime to High Density and High Radiation Loss

In the RS plasmas, a large volume configuration (V_p=75-80 m^3) with a small outer gap (Δ=8-16 cm) between the plasma and the outside wall was used with the plasma current of I_p=1.0 MA, the toroidal magnetic field of B_T=2.5-2.9 T, the safety factor at the 95% flux surface of q_{95}=5.8-6.5 and triangularity of δ_x=0.43-0.45 as shown in Fig. 1. The high density (n_e/n_{GW}~0.8) and high confinement (HH_{y2}=1.4) RS plasmas were achieved in this configuration [8]. It is noted that the large fast ion loss is induced due to the toroidal ripple in this configuration. In the RS plasmas, Ne was puffed from the divertor region and D_2 gas was puffed from the plasma top. In the high β_p H-mode plasmas, a small volume configuration (V_p=55 m^3) was used for high power central heating with I_p=1.0 MA, B_T=3.6 T, q_{95}=6.2, δ_x=0.37. In the high β_p H-mode plasmas, Ar was puffed from outer baffle, because some fraction of Ar density is necessary in the main plasma for confinement improvement and D_2 gas was also puffed from the plasma top. The HFS pellets were injected with 120 m/s and 10 Hz from the plasma top. The radiation loss was measured with 3 sets of bolometer arrays.

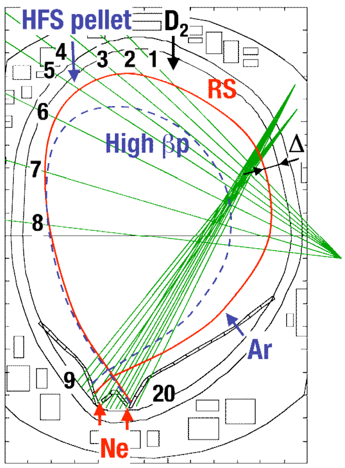

Fig. 1 Plasma configurations used in this study. Solid and dashed lines show the RS plasma and the high β_p H-mode plasma, respectively. Gas-puffing and pellet positions and diagnostic arrangement of bolometer arrays (ch1-20) are also shown.

Figure 2 summarizes the density dependence of HH_{y2}. In the RS plasmas, the high confinement of HH_{y2}=1.3 is obtained in the high density region above n_{GW} with NB fuelling only. In these discharges, NB and LHRF heating is applied to the large volume plasma with the small outer gap. With the small outer gap, the central density tends to increase rather than the central temperature during the confinement improvement. The central temperature is higher with the large outer gap (Δ=32 cm) than with the small outer gap at the same central density. It is noted that the direct loss of the fast ion supplied by NB is large due to a large toroidal ripple and the NB heating profile becomes off-axis with the small outer gap. These effects on the relationship between the central density and temperature should be investigated in future work. With Ne seeding, the total radiation loss is enhanced to a level greater than

90% of the net heating power with high confinement of HH_{y2}=1.1 at $\bar{n}_e/n_{GW}$=1.1, where NB heating is only applied. In order to suppress the impurity penetration into the main plasma, the edge density is increased by the D_2 gas-puffing in this plasma.

In the high β_p H-mode plasmas, $\bar{n}_e$ is increased up to $\bar{n}_e/n_{GW}$=0.92 with a small confinement degradation (HH_{y2}=0.96) by injecting multiple HFS pellets and Ar gas together with small D_2 gas-puffing. The Ar puffing assists to get high confinement at high density and high radiation loss up to 90% of the heating power. The density region of high confinement is limited below 0.7n_{GW} only with the HFS pellet injections [9]. The confinement degrades to HH_{y2}=0.75 at $\bar{n}_e/n_{GW}$=0.75 with the HFS pellet injections and strong D_2 gas-puffing. High confinement is obtained in the ELMy H-mode plasma without ITB by injecting Ar gas in the dome-top configuration, where the outer strike point is located on the divertor dome (I_p=1.2 MA, B_T=2.5 T and q_{95}=4.2) [11]. In the high β_p H-mode plasma, the high confinement is achieved with the divertor configuration.

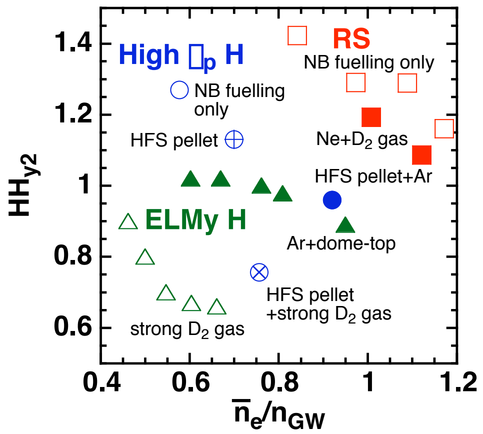

Fig. 2 HH_{y2} as a function of $\bar{n}_e/n_{GW}$. Squares : RS plasma. Circles : high β_p H-mode plasma. Triangles : ELMy H-mode plasma. Closed symbols show the data with impurity seeding.

The wave-forms of the high density and high confinement RS and high β_p H-mode plasmas with impurity seeding are shown in Fig. 3. In the RS plasma (Fig. 3 (a)), Ne was puffed during 5.5-5.8 s together with D_2 gas-puffing. The value of $\bar{n}_e$ starts to increase with ITB formation before the D_2 gas-puffing and reaches up to n_{GW}. The NB was injected using feedback control for the stored energy (W_{dia}). It is noted that the absorbed NB power is smaller than the injected power due to the large fast ion loss. The absorbed power is estimated to be 8.1 MW at t=7.0 s using an Orbit Following Monte-Carlo code. A mini collapse occurs at t=6.55 s and confinement slightly degrades from HH_{y2}=1.2 to 1.1. At t=7.1 s, another mini collapse occurs and plasma shrinkage is started, leading a current quench. Before the Ne puffing, ELM activity is clearly observed in the Dα intensity ($I_{D\alpha}$). However, after the Ne and D_2 gas-puffing, ELM activity disappears. The D_2 gas-puffing might affect the pedestal performance. Since the radiation (P_{rad}) from the divertor plasma is almost zero in the strong

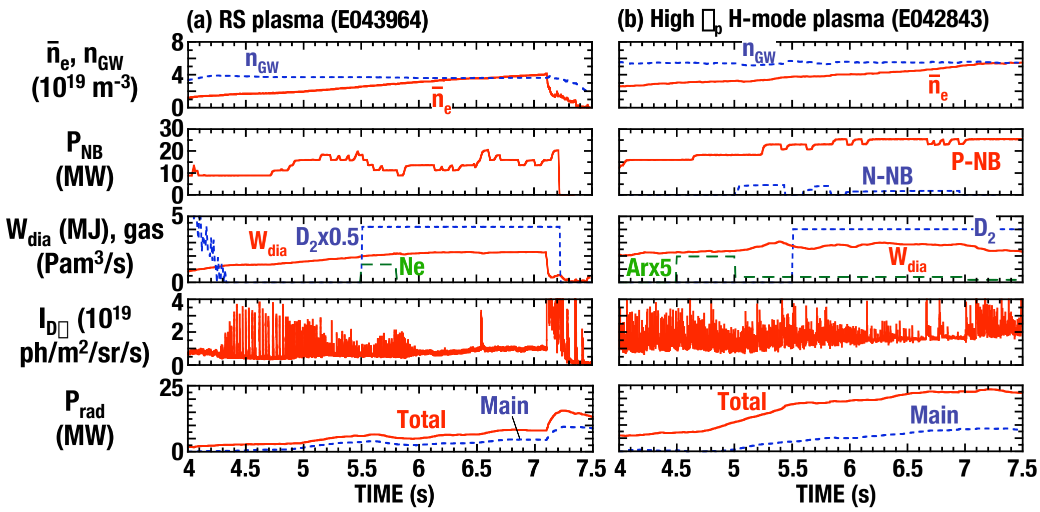

Fig. 3 Wave-forms of the impurity seeding plasmas. (a) Ne was injected in the RS plasma and (b) Ar was injected in the high β_p H-mode plasma.

ITB phase without Ne puffing, the divertor radiation is enhanced by Ne seeding. However, the radiation from the main plasma (~60% of the total radiation) is still larger than that from the divertor plasma, although the edge density is increased with D_2 gas-puffing for suppressing the impurity penetration. The total radiation reaches up to 90% of the net heating power. In this plasma, weak CuXXVI intensity is observed.

The wave-forms of the high density and high confinement high β_p H-mode plasma with Ar seeding are shown in Fig. 3 (b). The HFS pellets were injected from t=3.5 s and Ar was injected from t=4.5 s followed by small D_2 gas-puffing. The NB heating power of P_{NB}=20-30 MW from both positive and negative ion based NBs (P-NB and N-NB) was injected. The electron density increases and reaches n_{GW} around t=7.5s. The stored energy is almost kept at a constant value and confinement degradation at high density is suppressed until t=7 s. At t=7.1 s just after the end of N-NB injection, n=1 MHD mode appears and the confinement largely degrades, although the density continues to increase to $1.2n_{GW}$. Small ELMs are observed in $I_{D\alpha}$ during t=6.5-7 s, which is preferable for reduction of transient heat load onto the divertor plates. The change of the ELM amplitude was also observed in the ELMy H-mode plasma with Ar injection in the dome-top configuration [12]. The radiation losses in both main and divertor plasmas are enhanced after Ar injection. At t=6.95 s, the total radiation loss power reaches up to 90% of the heating power at $\bar{n}_e/n_{GW}$=0.92 with high confinement of HH_{y2}=0.96.

In the RS plasma, the density inside the ITB increases as shown in Fig. 4 (a). Although the edge density is smaller than $0.4n_{GW}$, $\bar{n}_e$ exceeds the n_{GW} due to the strong density ITB. The high $\bar{n}_e/n_{GW}$ is obtained due to the peaked density profile inside the ITB. The edge density increases by Ne and D_2 gas-puffing, while the edge temperature decreases. The same electron temperature is kept with higher density inside the ITB at t=7.0 s as shown in Fig. 4 (b). Before the Ne puffing (t=5.3 s), radiation loss is relatively flat as shown in Fig. 4 (c). The radiation profile becomes peaked one as the ITB becomes strong. At t=7.0 s after Ne puffing, the radiation loss from the main plasma is peaked. The radiation from the divertor is enhanced in the wide divertor region as shown in Fig. 4 (d).

In the high β_p H-mode plasma, the clear density ITB is formed and the peakedness increases in time after the Ar injection. In the Ar seeding H-mode plasma, slightly peaked density profile was observed at the dome-top configuration. However, clear density ITB is only

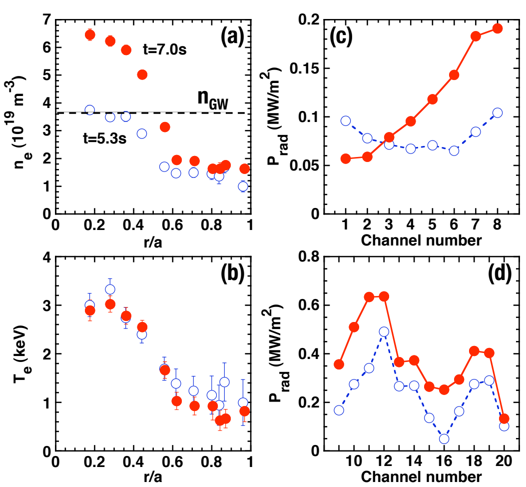

Fig. 4 Profiles of (a) electron density, (b) electron temperature, (c) radiation loss in the main plasma and (d) radiation loss in the divertor plasma in the RS plasma. Open and closed circles show the data at t=5.3 s and t=7.0 s, respectively.

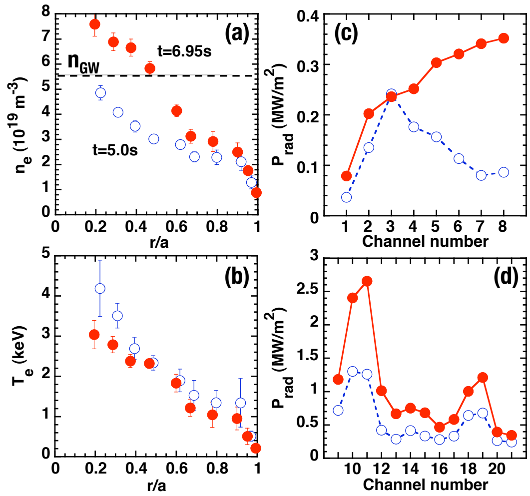

Fig. 5 Profiles of (a) electron density, (b) electron temperature, (c) radiation loss in the main plasma and (d) radiation loss in the divertor plasma in the high β_p H-mode plasma. Open and closed circles show the data at t=5.0 s and t=6.95 s, respectively.

observed in the high β_p H-mode plasma. At t=6.95 s with $\bar{n}_e/n_{GW}$=0.92, the ratio of the central density to the pedestal density reaches to about 3 as shown in Fig. 5 (a). Although the pedestal density is about half of n_{GW}, the central density becomes higher than n_{GW}. On the other hand, a flattening of the temperature profile is observed as shown in Fig. 5 (b). The radiation has a hollow profile before the Ar injection in the main plasma as shown in Fig. 5 (c). After the Ar injection, the central radiation increases. The divertor radiation is also enhanced in the wide region as shown in Fig. 5 (d).

3. Mechanisms of Confinement Improvement in High Density

In JT-60U, a possible feedback loop among the edge and core parameters has been proposed in the ELMy H- and high β_p H-mode plasmas [13], where improved core confinement (high β_p) enhances the edge pressure and the enhanced edge pressure improves the core confinement. In the high β_p H-mode plasma with the HFS pellets and Ar injections, the electron temperature at the pedestal top is higher than that in the ELMy H-mode plasmas without ITB at the same pedestal density as shown in Fig. 6 (a). Although the pedestal pressure is lower with Ar injection than with the HFS pellet injection or type II ELM regime, it enhances with Ar injection compared to that in the ELMy H-mode plasmas without ITB, where the confinement degradation is observed in the high density. After the confinement degradation (t>7s), the pedestal temperature decreases to the same level as in the ELMy H-mode plasmas without ITB. On the other hand, the pedestal pressure is smaller in the RS plasma without Ne and D_2 gas-puffing than in the ELMy H-mode plasmas without ITB. By Ne and D_2 gas-puffing, the pedestal density increases with small reduction of the pedestal temperature. The pedestal pressure is enhanced to the same level as that in the ELMy H-mode plasma without ITB.

The pedestal β_p is enhanced with the total β_p in the high β_p H-mode plasma as shown in Fig. 6 (b). The parameter-linkage between the edge and core plasmas is consistent with no Ar injection case, which indicates that the confinement improvement is not ascribed to only core confinement enhancement such as due to ITG mode suppression. Simple model [14] indicates that ITG mode seems to be suppressed due to density peaking and high Z_{eff} in this plasma. In the Ar seeded H-mode plasma without ITB, the ITG mode was not suppressed [15] because the peaking of the density profile is not strong. In the high β_p H-mode plasma, the high confinement is terminated by n=1 MHD mode located around the ITB. During the confinement degradation, the pedestal β_p also decreases with the total β_p. The change of the pedestal parameters such as density and temperature induced by the HFS pellet and Ar injections could be related to the trigger of the positive feedback loop for higher pedestal β_p and higher total β_p. The ITB degradation due to the MHD mode could be related to the trigger of the negative feedback loop. During the confinement degradation, the peaking of the density

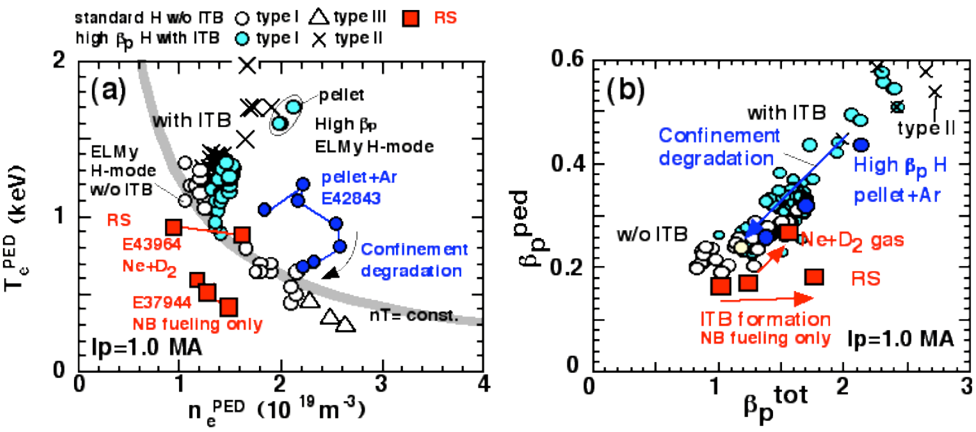

Fig. 6 (a) nT diagram at pedestal. (b) Relationship between pedestal β_p and total β_p.

profile still continues, while the temperature profile becomes further flat, indicating that ITG mode tends to be suppressed even during the confinement degradation. The ITG mode might affect to the particle transport rather than the energy transport. In the RS plasma, the pedestal β_p is almost kept at constant value, and the parameter-linkage between the edge and core plasmas is weak without Ne and D_2 gas-puffing. By Ne and D_2 gas-puffing, the pedestal β_p increases with the total β_p as observed in the H-mode plasmas. However, the pedestal β_p is kept at the same value as that with the degraded confinement in the high β_p H-mode plasma. The confinement improvement is mainly ascribed to core confinement enhancement due to the strong ITB in the RS plasma.

4. Radiation Loss Profile

The impurity transport is analyzed at t=7.0 s in the RS plasma (Fig. 3 (a)) and at t=6.95 s in the High β_p H-mode plasma (Fig. 3 (b)). The density profiles of the seed impurity are estimated using the 1-D transport calculation in the main plasma, in order to estimate the radiation profile from the seed impurity. The Ne density profile is assumed to be the same as electron density based on the previous observations [10]. The profile of the Ar density is evaluated based on the soft x-ray profile [6] using ADAS database [16]. The absolute values of Ne and Ar densities are determined by Bremsstrahlung measurements.

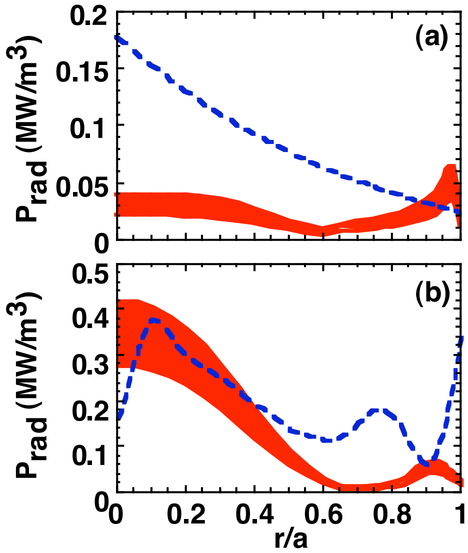

Fig. 7 Radiation loss profile in (a) RS plasma and (b) high β_p H-mode plasma. Dashed lines show the radiation profiles evaluated from the measurements by Abel inversion technique. Solid lines show calculated radiation from seed impurity (Ne or Ar).

In the RS plasma, the fraction of the Ne density to electron density is evaluated to be 2% and Z_{eff} exceeds 5 in the plasma center. The fuel purity defined by n_D/n_e is estimated to be about 0.5. The radiation loss profile evaluated from the measurements with the bolometer arrays by Abel inversion technique is peaked as shown in Fig. 7(a). However, the Ne radiation profile calculated with 1-D transport code is not so peaked as the measurement, and the absolute value is smaller than the measurement. Since the radiation from the intrinsic carbon (C) impurity is localized in the edge region, the core radiation can not be explained by radiation from Ne and C. In this plasma, CuXXVI line intensity was observed, indicating the metal impurity accumulation. The radiation loss from Cu might be largely contributed in the core plasma. Further optimization is necessary for high radiation fraction without metal impurity accumulation.

In the high β_p H-mode plasma, measured radiation profile is also peaked in the main plasma as shown in Fig. 7 (b). The Ar density calculated consistently with the soft x-ray profile is more peaked by a factor of 2 than the electron density profile. The Ar accumulation is weak compared with the neoclassical prediction. The fraction of the Ar density to the electron density is evaluated to be about 1% in the plasma center and 0.5% in the edge region. The value of Z_{eff} also exceeds 5 in the plasma center. The fuel purity is estimated to be about 0.6. The radiation profile calculated for Ar is the same level as the measurement in the central region as shown in Fig. 7 (b). However, the radiation from Ar is more peaked than the measurement and the radiation can not be explained by the radiation from Ar in the region of r/a=0.5-0.9. The radiation from C and oxygen (O) is localized in the edge region. Therefore, the radiation in r/a=0.5-0.9 can not be explained by the radiation from C and O. Origin of the radiation in this region should be investigated in future work.

Ar transport is also analyzed together with the intrinsic impurity C transport using the 2-D fluid code UEDGE [17] in the divertor and SOL plasmas for the high β_p H-mode plasma [18]. The carbon yield rate is set to be a Haasz yield for both physical and chemical sputtering. The Ar density at the core-edge boundary (96% flux surface) is scanned in the range of $(n_{Ar}/n_e)_{core\text{-}edge}$=0.5-1%. The total radiation loss power is calculated to be 7.2 MW with 1.2 MW from Ar, 5.4 MW from C and 0.6 MW from D at $(n_{Ar}/n_e)_{core\text{-}edge}$=0.5%. The value of $(n_{Ar}/n_e)_{core\text{-}edge}$=0.5% is consistent with the 1-D transport calculation in the main plasma. The calculated radiation profile with $(n_{Ar}/n_e)_{core\text{-}edge}$=0.5% is similar to the measured profile as shown in Fig. 8. However, the absolute value is smaller by a factor of 2 than the measurement. By increasing the Ar density, the peak in the outer divertor increases to the same level as measurement, while the peak in the inner divertor is almost constant. Since the drift influences the in-out asymmetry [19], the drift effects on the radiation profile should be investigated to reproduce the measurement by the calculation in future work. Furthermore, the large radiation at edge channels viewing the SOL plasma is often observed in the high triangularity configuration, [20]. However, it can not be reproduced by the calculation. Since effect of the secondary sepratrix near upper inside corner is strong in the high triangularity configuration, this effect on the radiation should be also investigated in future work.

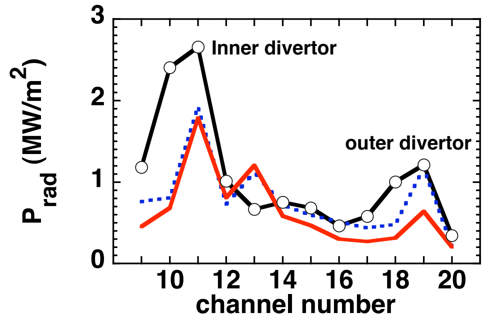

Fig 8 Comparison of divertor radiation loss between calculation and measurement. Solid and dotted lines show the calculations with $(n_{Ar}/n_e)_{core\text{-}edge}$ of 0.5 and 0.93%, respectively.

5. Discussion of Applicability to Fusion Reactor

Applicability of the impurity seeding to a fusion reactor with a peaked density profile is discussed. The peaked density profile inside the ITB has an advantage for high fusion power, but has a disadvantage for impurity accumulation [6]. Acceptable density peaking is investigated with Ar seeding using the A-SSTR2 parameters [1] ; I_p=12 MA, B_T= 11 T, R_p=6.2 m and a_p=1.5 m. Figure 9 shows pedestal density normalized by n_{GW} and HH_{y2} necessary for achieving a fusion power of 4 GW and radiation loss power in the main plasma side of about 400 MW. The Ar density of about 0.5% of the electron density is typically necessary in the plasma edge region for 400 MW radiation loss. The Ar density fraction is the same level as that obtained in the high β_p H-mode plasma. The electron and ion temperature profiles are assumed to have the ITB structure with the central temperatures of 30 keV. The pedestal density can be reduced below n_{GW} with $n_e(0)/n_e$(ITB-foot)>2 in the case of $n_{Ar}(0)/n_{Ar}$(ITB-foot)~1-2$\times n_e(0)/n_e$(ITB-foot). In this case, since the radiation loss in the core plasma is not large, required HH_{y2} gradually

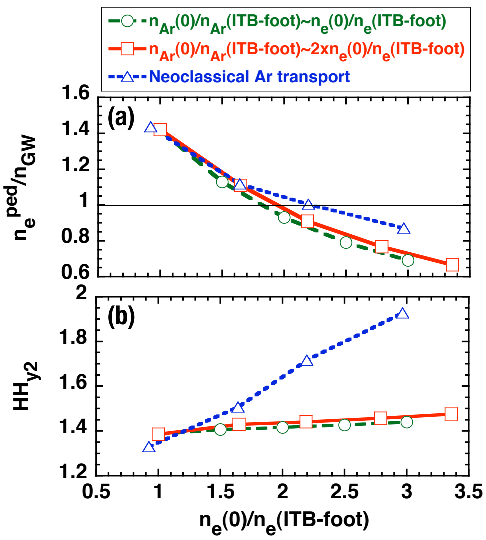

Fig. 9 Pedestal density normalized by n_{GW} and HH_{y2} required for 4 GW fusion power and 400 MW radiation loss as a function of density peaking.

increases with $n_e(0)/n_e$(ITB-foot). This analysis indicates that the density peaking can be acceptable with the Ar accumulation stronger by a factor of 2 than electron. On the other hand, in the case of neoclassical Ar transport case, higher pedestal density and higher HH_{y2} are necessary due to intensive impurity accumulation ($n_{Ar}(0)/n_{Ar}$(ITB-foot)~$8\times n_e(0)/n_e$(ITB-foot)). In addition, smaller edge n_{Ar} is necessary in this case, and the strong impurity shielding is important in the case of strong impurity accumulation. The density peaking is not acceptable with neoclassical impurity accumulation.

It is important to investigate whether the peaked density profile can be obtained under the reactor relevant conditions of electron heating and small central fueling. When the NB heating is switched to ECRF heating after the strong ITB formation in the RS plasma, the strong density ITB is maintained with small central fueling [21]. Even in the case that the ITB is formed with the small central fueling and electron heating using ECRF and N-NB injections, the density ITB is formed with temperature ITB.

6. Summary

Compatibility of advanced tokamak plasmas with high density and high radiation loss has been investigated in both reversed shear (RS) and high β_p H-mode plasmas of JT-60U. The high $\bar{n}_e/n_{GW}$ is obtained due to a peaked density profile inside the ITB. In the RS plasma, total radiation loss reaches up to 90% of the net heating power with high confinement (HH_{y2}=1.1) at high density ($\bar{n}_e/n_{GW}$=1.1) with Ne seeding. However, the radiation from Ne is not largely contributed to the radiation in the central region. Further optimization for high radiation loss operation without metal impurity accumulation is necessary. In the high β_p H-mode plasma, high confinement (HH_{y2}=0.96) is maintained at high density ($\bar{n}_e/n_{GW}$=0.92) with high radiation loss fraction (f_{rad}~0.9) by utilizing HFS pellets and Ar injections. Ar is accumulated inside the ITB and the radiation in the central region is ascribed to Ar. The impurity transport analyses indicate that core radiation loss from Ar impurity more accumulated by a factor of 2 than the electron can be compensated with slightly enhanced confinement in a fusion reactor.

References

[1] S. Nishio et al., Proc. 18th Int. Conf. on Fusion Energy 2000 (Sorrento, 2000) (Vienna:IAEA) CD-ROM file IAEA-CN-77/FTP2/14.
[2] H. Urano et al., Plasma Phys. Control. Fusion, **44** (2002) 11.
[3] J. Ongena et al., Nucl. Fusion, **44** (2004) 124.
[4] H. Takenaga et al., Fusion Science and Technology, **42** (2002) 327.
[5] G. Jackson et al., Nucl. Fusion, **42** (2002) 28.
[6] H. Takenaga et al., Nucl. Fusion, **43** (2003) 1235.
[7] R. Dux et al., Nucl. Fusion, **44** (2004) 260.
[8] S. Ide et al., Plasma Phys. Control. Fusion, **44** (2002) L63.
[9] H. Takenaga and the JT-60 Team, Phys. Plasmas, **8** (2001) 2217.
[10] H. Kubo et al., J. Nucl. Mater., **313-316** (2003) 1197.
[11] H. Kubo et al., Phys. Plasmas, **9** (2002) 2127.
[12] S. Higashijima et al., J. Nucl. Mater., **313-316** (2003) 1123.
[13] Y. Kamada et al., Plasma Phys. Control. Fusion **44** (2002) A279.
[14] H. Nordman et al., Nucl. Fusion, **30** (1990) 981.
[15] K.W. Hill et al., Proc. 19 th Int. Conf. on Fusion Energy 2002 (Lyon, 2002) (Vienna:IAEA) CD-ROM file IAEA-CN-94/EX/P2-03.
[16] SUMMERS, H. P., JET-IR 06, JET Joint Undertaking, Culham (1994).
[17] T. D. Rognlien et al., Contrib. Plasma Phys., **34** (1994) 362.
[18] H. Takenaga et al., submitted to J. Plasma Fusion Res.
[19] G. D. Porter et al., J. Nucl. Mater. **313-316** (2003) 1085.
[20] S. Konoshima et al., J. Nucl. Mater. **313-316** (2003) 888.
[21] H. Takenaga and the JT-60 team, Proc. 30th Eur. Conf. (St. Petersburg, 2003) O-1.1A, http://epsppd.epfl.ch/StPetersburg/PDF/O1_001A.PDF